Enhanced Virtual Inertia Control Based on Derivative Technique to Emulate Simultaneous Inertia and Damping Properties for Microgrid Frequency Regulation

THONGCHART KERDPHOL[1], **(Member, IEEE),**
FATHIN SAIFUR RAHMAN[1], **(Student Member, IEEE),**
MASAYUKI WATANABE[1], **(Member, IEEE),**
YASUNORI MITANI[1], **(Member, IEEE),**
DIRK TURSCHNER[2], **AND HANS-PETER BECK**[2]

[1]Department of Electrical and Electronic Engineering, Kyushu Institute of Technology, Kitakyushu 804-8550, Japan
[2]Institute of Electrical Power Engineering and Energy Systems, Clausthal University of Technology, 38678 Clausthal-Zellerfeld, Germany

Corresponding author: Thongchart Kerdphol (kerdphol@ieee.org)

ABSTRACT Virtual inertia control is considered as an important part of microgrids with high renewable penetration. Virtual inertia emulation based on the derivative of frequency is one of the effective methods for improving system inertia and maintaining frequency stability. However, in this method, the ability to provide virtual damping is usually neglected in its design, and hence, its performance might be insufficient in the system with low damping. Confronted with this issue, this paper proposes a novel design and analysis of virtual inertia control to imitate damping and inertia properties simultaneously to the microgrid, enhancing frequency performance and stability. The proposed virtual inertia control uses the derivative technique to calculate the derivative of frequency for virtual inertia emulation. Trajectory sensitivities have been performed to analyze the dynamic impacts of the virtual inertia and virtual damping variables over the system performance. Time-domain simulations are also presented to evaluate the efficiency of the virtual damping and virtual inertia in enhancing system frequency stability. Finally, the efficiency and robustness of the proposed control technique are compared with the conventional inertia control under a wide range of system operation, including the decrease in system damping and inertia and high integrations of load variation and renewable energy.

INDEX TERMS Frequency stability, isolated microgrid, virtual inertia regulation, virtual synchronous machine.

I. INTRODUCTION

Recently, the transition in electricity from centralized generation to distributed/decentralized generation (DG) has made microgrids attractive and suitable for integrating renewable energy sources (RESs). The microgrid infrastructure has proven to be an alternative strategy for solving the challenges of the energy crisis and environmental concerns, as it consists of DG/RESs, energy storage systems (ESS), and distributed loads [1]. With the rising share of RESs-based generation, it raises the new stability issues in regulating the microgrid.

One of the major problems is the lack of system inertia and damping owing to the replacement of traditional generations (i.e., synchronous generators) by RESs-based generation. The main reason for system inertia reduction is because of the converter/inverter that is usually used to connect the RESs to the microgrids. The inverter/converter does not possess any inertia or damping properties, leading to the degradation of system inertia and damping, larger frequency excursion, and system instability and collapse, see for an example [2]. On the contrary, high system inertia and damping generated by the

synchronous generators are required to attenuate the system dynamics and decrease frequency deviation of the system, so that the system instability, undesirable load or generation-shedding, cascading outages, and power blackouts could be prevented. Thus, dynamic stability in the presence of low system inertia and damping caused by RESs penetration is becoming the main concern for today and future microgrid design, operation, and control, as its stability margin is reduced.

To address these stability issues, a new inertia control scheme called virtual synchronous machine (VISMA) [3]–[5] or virtual synchronous generator (VSG) [6] is designed to imitate virtual inertia power based on the dynamic behavior of synchronous generators, improving system performance and stability. The virtual inertia control concept is constructed by the inverter, short-term energy storage system (ESS), and proper control technique. Recently, several researchers have paid more attention to investigate these issues. Thus, there are many types of virtual inertia control, depending on the control objectives. The research groups in [4]–[6] designed the virtual inertia control to imitate the dynamic and static characteristics of synchronous generators, improving system performance. D'Arco *et al.* [7] ensured that virtual inertia control is able to provide stable operation of microgrids in both islanded and grid-connected operations, maintaining robustness of operation. The comparison of dynamic behavior between virtual inertia control and droop control is investigated in [8]. Hirase *et al.* [9] analyzed the resonance effect in microgrids using virtual inertia control in response to frequency stabilization. The stability assessment technique is discussed in regards to multiple virtual inertia control units [10]. The concept of synchronverter is also proposed in [11] to mimic the behaviour of synchronous generators for inertia control. For more details, interested readers can find the literature reviews and past research achievement on virtual inertia control in [12] and [13].

From the past until now, significant phenomena that cause microgrid instability and power blackout are frequency instability, rotor angle instability, and voltage instability. Focusing on frequency stability/regulation, virtual inertia control based on the derivative technique (derivative of frequency: df/dt) [14]–[16] is one of the effective approaches for imitating virtual inertia power, improving system inertia and frequency stability. Numerous publications have designed virtual inertia control based on the derivative approach for the enhancement of frequency stability [14]–[20]. In [14]–[16], the derivative method-based inertia control was applied to the HVDC interconnected system, improving frequency stability. Alhejaj and Gonzalez-Longatt [17] investigated the impact of derivative technique-based inertia control for enhancing frequency response. Kerdphol *et al.* [18] proposed the model predictive control to control the inertia power in derivative method-based inertia control. Kerdphol *et al.* [19] applied the derivative technique-based virtual inertia control to augment frequency performance of HVAC systems. Kerdphol *et al.* [20] combined the robust

theory and virtual inertia control to reduce frequency oscillation during high RESs penetration. Recently, Fang *et al.* [21] investigated the frequency derivative-based inertia improvement considering the effect of frequency measurement. Stability issues in response to this technique have been identified in [22]–[26]. However, most of the published research work in this area [14]–[20] neglect the design of virtual damping, which is important in providing additional damping property to the microgrids. The lack of the virtual damping can lead to an insufficient performance of virtual inertia control in the microgrids with low inertia and damping. This problem would also be exacerbated in the situation of low load damping factor of the microgrid during small power consumption, causing the system instability and collapse [27]. Moreover, there is no consideration has been paid in the literature to deal with this issue in the application based on the derivative technique. To fill in this research gap and overcome the problem, the new modeling of derivative technique-based virtual inertia control is strongly required to augment system damping, inertia, and frequency performance/stability.

This paper proposes a novel design and analysis of virtual inertia control to imitate damping and inertia properties simultaneously into the microgrid, enhancing frequency stability and robustness under a wide range of system operation. The virtual inertia part is established by using the derivative technique-based virtual inertia emulation technology presented in [14]–[16]. The virtual damping part is calculated based on the frequency deviation of the system in regards to fast settling/stabilizing time of the system. Trajectory sensitivities have been presented to analyze the dynamic impacts of virtual damping and virtual inertia variables. Finally, the efficiency of the proposed method is confirmed by the simulation study.

The novelty of this work is summarized as: (1) the enhanced derivative technique-based virtual inertia control strategy that enables simultaneous emulation of virtual inertia and damping is proposed, improving both system inertia and damping to meet frequency regulation requirements; (2) the dynamic effects of virtual damping and virtual inertia are analyzed and validated by using the eigenvalue analysis and time-domain simulation, obtaining a new trade-off between frequency transient/deviation and settling time; (3) compared with the virtual inertia control literatures in [14]–[20], the proposed strategy gives a better frequency stability and performance to the microgrid, which is expected to integrate more RESs, and thus, the lack of system inertia and damping issue could be solved and preventing instability and power blackout. In this work, the dynamic effects of both virtual damping and virtual inertia have been clearly investigated so that the virtual inertia control could be more optimally utilized in the power system.

The remainder of this manuscript is arranged as; Section II explains a brief review of frequency regulation in regards to inertia control. The dynamic of the microgrid based on frequency regulation is discussed. Section III proposes the new modeling of derivative technique-based virtual

inertia control. In Section IV, the effects of virtual damping and virtual inertia are investigated. The microgrid frequency response is examined through the severe situations in normal and extremely low system inertia and damping. Finally, the conclusions are offered in Section V.

II. SYSTEM CONFIGURATION

A. FREQUENCY REGULATION IN REGARDS TO INERTIA CONTROL

Frequency stability issue, as a result of the unbalance between load consumption and power generation, is one of the most concerning problems in microgrid design, operation, and control. In traditional power systems (i.e., synchronous generator-based power system), the inertia and damping properties generated from the rotor of synchronous generators offer an imperative role in regulating frequency stability during the contingency (e.g., RESs/load variation). The relationship between generated power, load power, system inertia, system damping, and frequency deviation is defined by the swing equation as [28]:

$$\Delta P_m - \Delta P_L = 2Hs(\Delta f) + D(\Delta f) \tag{1}$$

where f means the frequency of the system, Δf means the deviation of system frequency, ΔP_m means the generated power change from the synchronous generator, ΔP_L means the load power change, H means the system inertia, D means the system damping.

To regulate the frequency stability at a nominal value (i.e., 50 or 60 Hz) under a wide range of microgrid operation, three main control units; (1) inertia (initial) control, (2) primary control, and (3) secondary control, are usually designed to deal with the contingency as shown in Fig. 1. For a full detailed explanation of these control processes, it can be found in [28] and [29]. Focusing on inertia response, the stored inertia power (i.e., kinetic energy) in the rotors of the synchronous generators will counteract the imbalance through the inertia control until before the primary control is fully activated. The relationship between the inertia of the synchronous generator and inertia of the microgrid can be determined as [28], [29]:

$$H = \sum_i (H_{SGi} S_{SGi}) / S_{MG} \tag{2}$$

where S_{SG} means the rated power of the synchronous generator, and S_{MG} means the rated microgrid power.

Recently, in microgrids, the synchronous generators have been replaced by the inverter/converter-based RESs. Hence, the response of system inertia (H) and system damping (D), typically during 1-10s is significantly decreased. Accordingly, the rate of change of frequency or derivative of frequency (df/dt) of the microgrids increases, leading to rapid frequency deviation, larger frequency drop/dip, system instability, and in the worst case; a rapidly cascading failure or power blackout. It is noted that during the short time interval of 1-10s, the primary and secondary control units are not effective enough to counteract the contingency
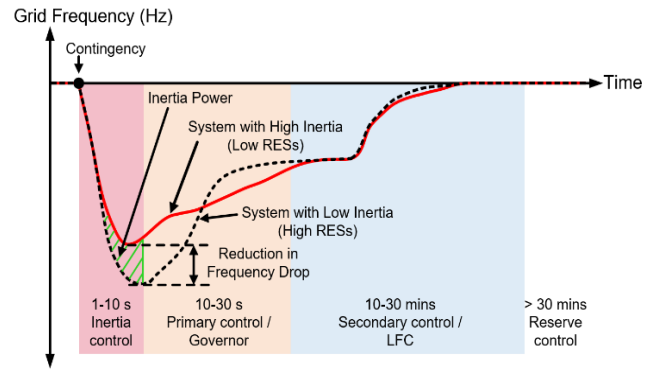

FIGURE 1. Time intervals of frequency response during a contingency.

(see Fig. 1), especially under the severe situations of low system inertia and damping caused by RESs penetration.

B. DYNAMIC MODELING OF MICROGRID FOR FREQUENCY REGULATION AND ANALYSIS

To obtain the multi-source nature of microgrid, the studied microgrid in Fig. 2a contains several kinds of generation system, with different types of load. The main thermal power station has 15 MW of installed capacity, representing a traditional synchronous generator-based generation. The generated electricity is consumed by 10 MW of commercial-industrial loads and 5 MW of residential loads. The system has 8.5 MW installed capacity of the wind farms and 7.5 MW installed capacity of the solar power plants. None of them equipped with inertia or damping emulation controller. Hence, the renewable power generations will significantly change the microgrid operating point and reducing system inertia and damping property, affecting system stability and performance. To solve this problem, energy storage systems (ESS) of 4.5 MW are installed in the microgrid. The system base is 15 MW. The communication network (dotted line) is applied for exchanging information and status. The frequency control network (dash line) is used for control instruction of inertia, primary, and secondary control units. The power network (solid line) is applied for delivering the electrical power to the loads in the microgrid.

To analyze frequency stability effectively, the dynamic model of the studied microgrid in Fig. 2b is developed for frequency study and analysis. To obtain the physical system dynamics, the generation rate constraint (GRC) for the governor unit, dead band for the turbine unit, and time delay for the secondary control or load frequency control (LFC) unit are considered, creating an accurate frequency perception and system non-linearity [28], [29]. In this study, the GRC is specified as 12% p.u. MW/min. The dead band limit is specified as 0.06% ($\pm$0.035 Hz). The time delay is specified as 2 s. Three main control units (i.e., inertia control, primary control, and secondary control) are applied to maintain system frequency stability during the contingency. The inertia control-based ESS is responsible for balancing the mismatch
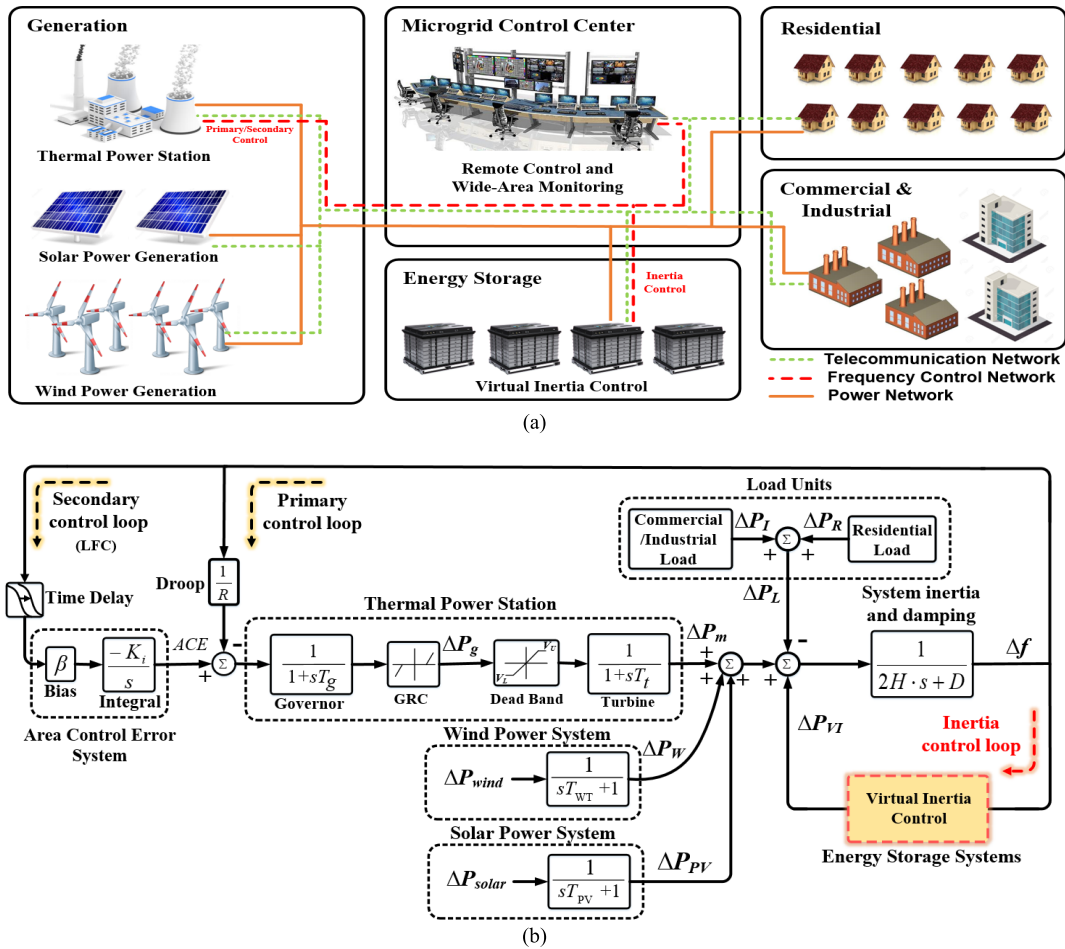
FIGURE 2. The studied microgrid system: (a) Conceptual structure, (b) Dynamic structure for frequency response analysis.

power at 1-10s. The primary control unit (i.e., the governor) is responsible for stabilizing the system frequency to a new steady-state value within 10-30s. The secondary control (also known as load frequency control: LFC) based on area control error (ACE) is responsible for recovering the system frequency to its nominal value within 10-30 minutes. On the contrary, because the RESs (wind and solar power systems) and domestic loads (industrial and commercial-residential loads) do not participate in the frequency regulation, they are considered as the disturbances/uncertainties to the microgrid. Based on [14]–[16] and [27]–[32], the simplified model of the studied microgrid (i.e., low-order dynamic model) presented in Fig. 2b is sufficient for frequency stability study and analysis. Nevertheless, [27] compared frequency response obtained using the simplified model and the detailed model of the microgrid. It is confirmed that the simplified model has a good accuracy under a wide range of operating conditions. Thus, the simplified model used in this work is accurate enough for frequency stability study and analysis. Pertinent model parameters are displayed in Table 1.

Considering the dynamic effects of generations and loads including inertia, primary, and secondary control

(from Fig. 2b), the system frequency deviation is obtained as:

$$\Delta f = \frac{1}{2Hs + D}(\Delta P_m + \Delta P_W + \Delta P_{PV} + \Delta P_{VI} - \Delta P_L) \tag{3}$$

where

$$\Delta P_m = \frac{1}{1 + sT_t}\left(\Delta P_g\right) \tag{4}$$

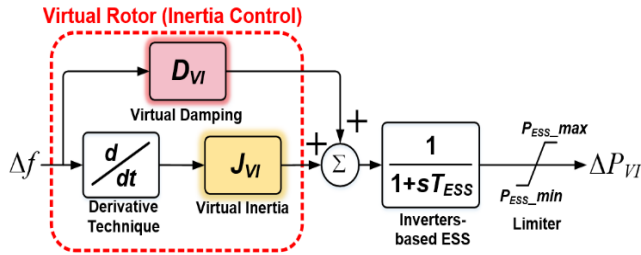$$\Delta P_g = \frac{1}{1 + sT_g}\left(ACE - \frac{1}{R}\Delta f\right) \tag{5}$$

$$ACE = \frac{K}{s}\left(\beta \cdot \Delta f\right) \tag{6}$$

$$\Delta P_W = \frac{1}{1 + sT_{WT}}\left(\Delta P_{wind}\right) \tag{7}$$

$$\Delta P_{PV} = \frac{1}{1 + sT_{PV}}\left(\Delta P_{solar}\right) \tag{8}$$

$$\Delta P_L = P_I + P_R \tag{9}$$

where *ACE* means the area control error. ΔP_W means the generated power from the wind system. ΔP_{wind} is the initial wind power change. ΔP_g is the generated power from the turbine system. ΔP_{solar} is the initial solar power change.

FIGURE 3. The dynamic structure of derivative technique-based virtual inertia control to imitate virtual damping and inertia.

ΔP_{PV} means the generated power from the solar system. ΔP_I is the commercial-industrial load power. ΔP_R is the residential load power. ΔP_{VI} is the virtual inertia power. Note that ΔP_{VI} will be explained in the next section (see (15)).

To perform the detailed investigation for the studied microgrid, the complete state-space model representation of the system could be calculated as:

$$\dot{x} = Ax + B_1 w + B_2 u \tag{10}$$

Considering the block diagram of Fig. 2b, the coefficients and state variables of the proposed state-space model in (10) is evaluated as follows:

$$x^T = \begin{bmatrix} \Delta f & \Delta P_m & \Delta P_g & \Delta P_{ACE} & \Delta P_{VI} & \Delta P_W & \Delta P_{PV} \end{bmatrix} \tag{11}$$

$$w^T = \begin{bmatrix} \Delta P_W & \Delta P_{PV} & \Delta P_I & \Delta P_R \end{bmatrix} \tag{12}$$

$$u^T = \begin{bmatrix} \Delta P_{VI} \end{bmatrix} \tag{13}$$

Therefore, the complete state-space equation of the system is determined as (14), shown at the bottom of this page.

III. VIRTUAL INERTIA CONTROL BASED ON DERIVATIVE TECHNIQUE FOR SIMULTANEOUS EMULATION OF VIRTUAL INERTIA AND DAMPING

This section explains a novel concept, design, and modeling of derivative technique-based virtual inertia control for simultaneous emulation of virtual inertia and virtual damping, enhancing frequency performance and avoiding system instability/collapse owing to the lack of system damping and inertia. The main design objective is to simultaneously

provide the virtual damping and virtual inertia to support the conventional synchronous generators in the situations of low system inertia and damping when the RESs are highly penetrated to the microgrid. This concept can be established by the short-term ESS, inverter, and proper inertia control technique. The proposed control technique is designed to operate independently of other control units, such as primary and secondary control. Thus, the energy contained in ESS is fully used to improve the system frequency stability in terms of steady-state and transient performance.

The dynamic modeling of the proposed technique is presented in Fig. 3. The virtual inertia part is established based on the inertia emulation technology using the derivative technique introduced in [14]–[16] to determine the rate of change of frequency (df/dt) for modifying the added power to a set-point of the microgrid during the contingency. The virtual damping part is developed for fast settling/stabilizing time based on the frequency deviation of the system. As a result, the active power via the inverter-based ESS is proportionally controlled using the df/dt. Hence, the virtual inertia power with damping property could be properly emulated into the microgrid, enhancing both system inertia and damping, as well as frequency stability. The low-pass filter is used to eliminate the noise issue and to get the accurate dynamics of inverter-based ESS (i.e., fast response characteristic). The limiter block is implemented to limit the ESS output power, representing the practical power response of the ESS. Accordingly, the proposed inertia control is able to contribute to the microgrid as if the ESS has inertia and damping properties similar to that of the conventional synchronous generator. Considering the capability of the proposed technique, it is worth to point that the proposed inertia control can achieve a better performance than the conventional virtual inertia control due to the designed flexible damping controller, which can achieve an optimal response in case of contingencies, especially under the severe circumstances of low system damping and inertia. Without the virtual damping emulation, there is no damping property in the conventional inertia control and the system damping is limited by its actual physical factors.

$$\dot{x} = \begin{bmatrix} \dfrac{-D}{2H} & \dfrac{1}{2H} & 0 & 0 & \dfrac{1}{2H} & \dfrac{1}{2H} & \dfrac{1}{2H} \\ 0 & -\dfrac{1}{T_t} & \dfrac{1}{T_t} & 0 & 0 & 0 & 0 \\ \dfrac{-1}{RT_g} & 0 & -\dfrac{1}{T_g} & \dfrac{1}{T_g} & 0 & 0 & 0 \\ \beta \cdot K_i & 0 & 0 & 0 & 0 & 0 & 0 \\ \dfrac{D_{VI}}{T_{ESS}} & 0 & 0 & 0 & \dfrac{-1}{T_{ESS}} & 0 & 0 \\ 0 & 0 & 0 & 0 & 0 & \dfrac{1}{T_{WT}} & 0 \\ 0 & 0 & 0 & 0 & 0 & 0 & \dfrac{-1}{T_{PV}} \end{bmatrix} x + \begin{bmatrix} 0 & 0 & \dfrac{-1}{2H} & \dfrac{-1}{2H} \\ 0 & 0 & 0 & 0 \\ 0 & 0 & 0 & 0 \\ 0 & 0 & 0 & 0 \\ 0 & 0 & 0 & 0 \\ \dfrac{1}{T_{WT}} & 0 & 0 & 0 \\ 0 & \dfrac{1}{T_{PV}} & 0 & 0 \end{bmatrix} w + \begin{bmatrix} 0 \\ 0 \\ 0 \\ 0 \\ \dfrac{J_{VI}}{T_{ESS}} \\ 0 \\ 0 \end{bmatrix} u \tag{14}$$
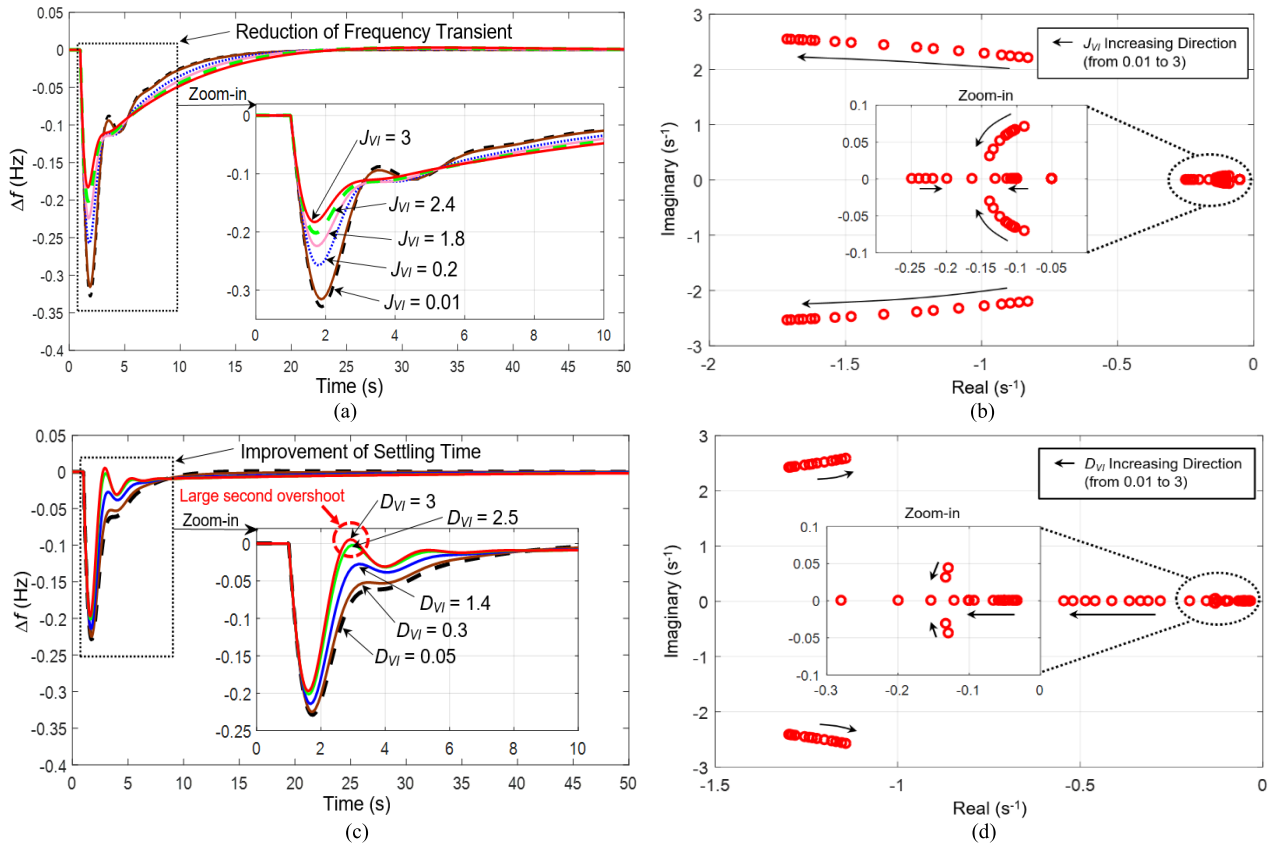
FIGURE 4. Stability analysis of different variables of virtual damping and virtual inertia over the system performance: (a) Effect of virtual inertia but no virtual damping, (b) Eigenvalue trajectory of the system with virtual inertia but no virtual damping, (c) Effect of virtual damping and virtual inertia, (d) Eigenvalue trajectory of the system with virtual inertia and virtual damping.

The dynamic equation or control law of the proposed control design can be expressed as:

$$\Delta P_{VI} = \frac{J_{VI}s + D_{VI}}{1 + sT_{ESS}} (\Delta f) \qquad (15)$$

where J_{VI} means the virtual inertia constant, D_{VI} means the virtual damping constant, T_{ESS} means the time constant of inverter-based ESS.

More detail and information about the equivalent mechanical model in regards to virtual inertia control studies can be found in [3]–[5], based on a specific type of virtual inertia control called VISMA.

IV. SIMULATION RESULTS AND DISCUSSION

We have carried out the analysis and simulations using MATLAB/Simulink software in parallel to the proposed control and development presented above. Results that confirm the proposed modeling of virtual inertia control are presented in this section. The simulations and analysis are focused on three parts. The first part is focused on the impacts of the virtual damping (D_{VI}) and virtual inertia (J_{VI}) including the system inertia and damping itself over the microgrid performance. The second and third parts are focused on the frequency stability assessment of the microgrid under the normal and critical operating situations caused by different

penetration levels of RESs and variation in residential and commercial-industrial loads. To determine the efficiency and robustness of the proposed control design, the results have been compared with the conventional derivative technique-based virtual inertia control designed in [14]–[20] and no virtual inertia control.

A. IMPACTS OF VIRTUAL DAMPING AND VIRTUAL INERTIA OVER MICROGRID PERFORMANCE

In this part, the time-domain simulation and eigenvalue analysis of the studied system are presented to evaluate the dynamic impacts of virtual damping (D_{VI}) and virtual inertia (J_{VI}) based on the small-signal stability point of view. To illustrate the microgrid behaviour over a wide range of parameter changes, the complete eigenvalue trajectory is presented. This section is divided into two sub-scenarios as follows: (1) the impact of virtual inertia; (2) the impact of virtual damping and virtual inertia.

Scenario 1: In this scenario, only the effect of the change in the virtual inertia constant values (J_{VI}) over the microgrid performance is considered. The test is performed by a step load change of 1.5 MW ($\Delta P_L = 0.1$ p.u.) at 1 s under the normal condition of high system inertia and damping. Fig. 4a shows the frequency deviation for different values
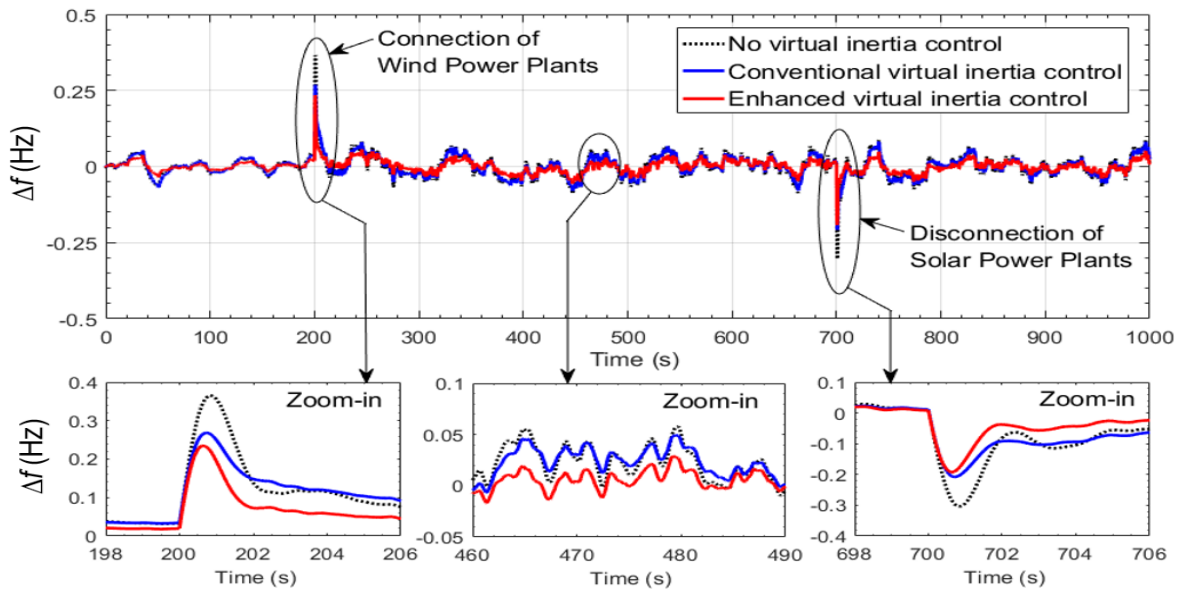
FIGURE 5. Frequency response of the microgrid under the normal operating situation of high system inertia and damping.

of J_{VI}. It is found that the key effect of increasing J_{VI} (from 0.01 to 3) is that the frequency transient and maximum frequency deviation significantly reduce, resulting in a better microgrid performance. It is confirmed by the eigenvalue trajectory of the system in Fig. 4b that after increasing J_{VI}, the negative real part of most eigenvalues move to the leftward region of the s-plane (i.e., stable region), improving frequency stability margin. However, Fig. 4a also shows the side effect of increasing virtual inertia constant value (J_{VI}). If the J_{VI} is increased too high (especially over 2), the microgrid frequency will need a longer time to settle. Thus, the side effect of increasing J_{VI} is that the settling/stabilizing performance of the system could be deteriorated, leading to a longer settling/stabilizing time. To overcome this issue, the study and analysis of virtual damping design are provided in the next scenario.

Scenario 2: This scenario is mainly focused on the effect of the changes in virtual damping constant values (D_{VI}) over the microgrid performance, while the effect of virtual inertia (J_{VI}) is simultaneously considered and fixed at the proper value of 1.6. Similarly, the test is performed by a step load change of 1.5 MW ($\Delta P_L = 0.1$ p.u.) at 1 s under the normal condition of high system inertia and damping. Fig. 4c shows the frequency deviation for different values of D_{VI}. Obviously, the advantage of emulating virtual damping to the microgrid system is the significant improvement of settling/stabilizing performance (less settling time) and the slight attenuation of frequency transient. It is confirmed by the eigenvalue trajectory in Fig. 4d that the negative real part of the system moves to the leftward region of the s-plane. However, the side effect of applying the high value of virtual damping can be observed in Fig. 4c and 4d. If the D_{VI} is increased too high (especially over 2), it could result in the

large second overshoot at 3 s (see cases of $D_{VI} = 2.5$ and 3 in Fig. 4c). This side effect is confirmed by Fig. 4d that the main negative imaginary part of the microgrid moves slightly toward the right side of the s-plane (i.e., unstable region) after applying the high values of D_{VI}. As a result, when virtual inertia and virtual damping are applied simultaneously, it is better to keep a smaller value of virtual damping (less than 1.5) and give the main responsibility of suppressing the frequency deviation in case of the contingency to the virtual inertia part.

B. FREQUENCY STABILITY ASSESSMENT UNDER HIGH SYSTEM INERTIA AND DAMPING PROPERTY

Scenario 3: This scenario represents a normal operating situation of the microgrid with low penetration of wind and solar generations (see Fig. 6a) and high power consumption of residential and commercial-industrial loads (see Fig. 6b). Both system inertia and damping are reduced 20% from their nominal values (see Table 1). To replicate the typical microgrid operation, the power fluctuations due to wind velocity, solar irradiance, and electrical load consumption are simultaneously applied to the microgrid. How the proposed inertia control regulates the microgrid frequency stability under the impact of high load power consumption with low RESs production is also examined in this scenario. For this scenario, the control parameters have been listed in Table 1.

Fig. 5 shows the microgrid frequency response under this scenario. Obviously, due to the connection of wind power plants at 200 s, it results in the huge frequency rise of +0.37 Hz in case of no virtual inertia control, +0.26 Hz in case of conventional inertia control, and +0.22 Hz (the lowest) in case of the proposed inertia control. Moreover, the conventional virtual inertia control yields longer settling time, which is almost the same as the case of no virtual
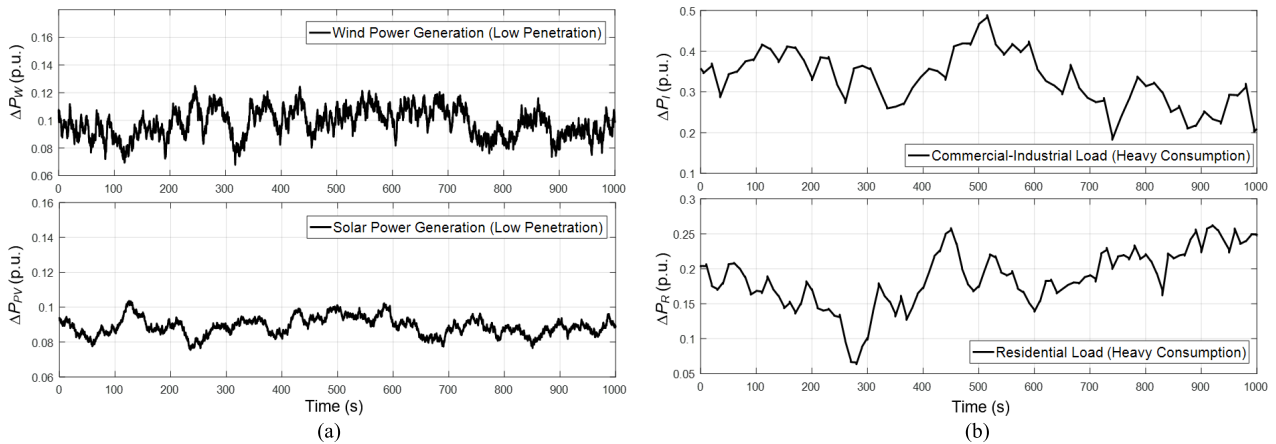
FIGURE 6. The considered power disturbances: (a) Low penetration of wind and solar energy (b) High consumption of commercial-industrial and residential loads.

inertia control due to the lack of virtual damping emulation. On the contrary, when the proposed inertia control is applied, the frequency rise has the lowest value with less settling/stabilizing time. This improvement is due to the capability of the proposed virtual inertia control to emulate virtual inertia and damping, simultaneously. During no contingency event, for example from 460 to 490 s, the proposed control technique could effectively regulate frequency deviation with the lowest value. This indicates the efficiency in maintaining stable microgrid operation. Following the disconnection of solar power plants at 700 s, it causes the frequency drop of −0.31 Hz in case of no inertia control, −0.21 Hz in case of conventional inertia control, and −0.17 Hz (the lowest) in case of the proposed inertia control. Similarly, both conventional inertia control and no inertia control give longer settling/stabilizing time due to the lack of damping emulation. By designing the virtual damping as in the proposed control technique, the stabilizing/settling time is significantly reduced, effectively enhancing frequency stability margin and resiliency of the microgrid. Fig. 7 illustrates the emulated virtual inertia power from the ESS for Scenario 3. The positive value indicates the charging power while the negative value indicates the discharge power. It is obvious that the ESS controlled by the proposed technique is greatly charged/discharged in response to the applied disturbances and contingencies.

Hence, the simulation results confirm that the proposed inertia control technique provides much better stability/performance in suppressing frequency deviation/transient excursion and improving system resiliency, specifically in settling/stabilizing time under the normal operating situation of the microgrid.

C. FREQUENCY STABILITY ASSESSMENT UNDER LOW SYSTEM INERTIA AND DAMPING

Scenario 4: In this situation, the robustness of the proposed control technique under the critical operating condition is examined. According to the frequency stability point of view,
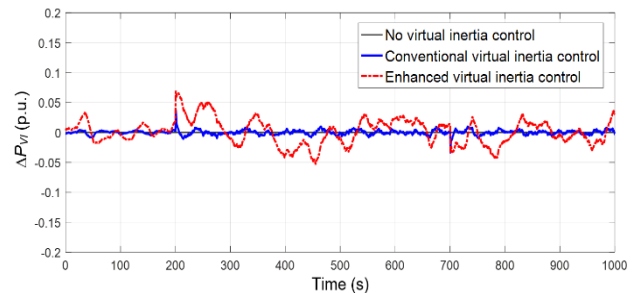
FIGURE 7. Power change of the ESS with virtual inertia and damping emulation for Scenario 3.

the worst operating situation of the microgrid is when the system operates at the maximum RESs power production (e.g. in this case, 90% of its installed capacities, see Fig. 9a) resulting in the extremely low system inertia (e.g. in this case, 80% reduction from its nominal value). To force more severe operating situation, the microgrid has the minimum load consumption (20% of its peak demand, see Fig. 9b) resulting in the extremely low system damping (e.g. in this case, 80% reduction from its nominal value). For this scenario, the related parameters have been listed in Table 1. This severe scenario is executed over a total time of 15 minutes. The necessity of applying the proposed inertia control for compensating the impacts of low system damping and inertia and achieving the stable frequency performance has been demonstrated in this scenario.

Fig. 8 reveals the system frequency stability under the critical scenario. With increasing penetration of RESs in this scenario (specifically after 200 s), it is obvious that the maximum frequency deviation of the microgrid significantly increases. In case of no inertia control, the microgrid completely fails to regulate the frequency stability, leading to the power blackout. In case of conventional inertia control, strong frequency peak/transient and larger frequency deviation can be observed during the connection of the wind farms
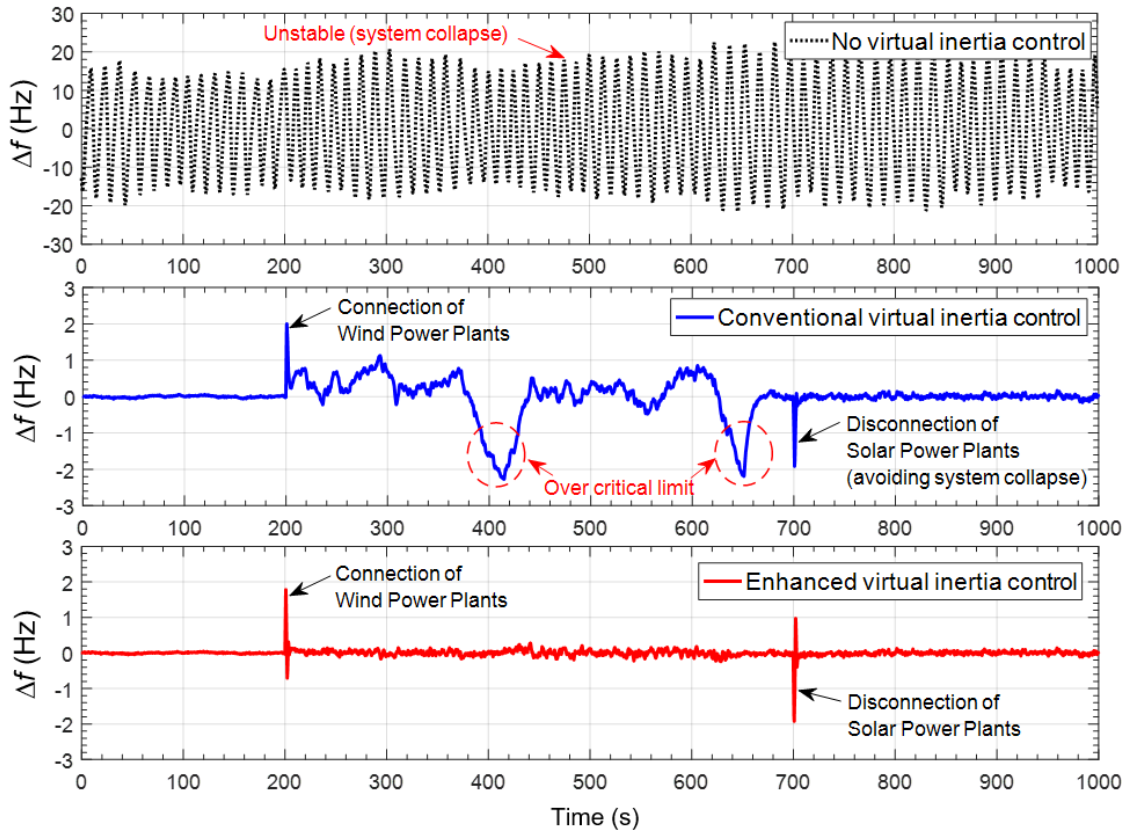
FIGURE 8. Frequency response of the microgrid under the extreme operating situation of low system damping and inertia.
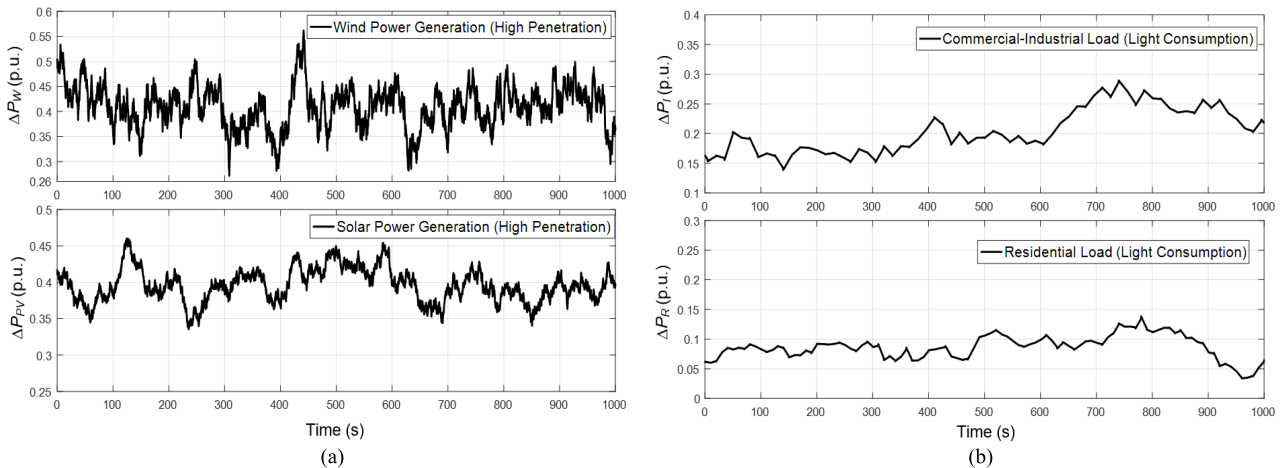

FIGURE 9. The considered power disturbances: (a) High integration of wind and solar energy (b) Low consumption of commercial-industrial and residential loads.

from 200 s (i.e., the period of maximum RESs power penetration). During no contingency event (from 201 to 699 s), the microgrid frequency in case of conventional inertia control severely oscillates over the frequency operating standard of ±1 Hz [33] twice due to the lack of system damping. This situation may lead to the instability and system collapse. To prevent such severe situation, the disconnection of solar

power plants at 700 s is required in case of conventional inertia control. On the contrary, it is obvious that the proposed virtual inertia control gives much smaller frequency transient and derives frequency deviation close to zero with smooth changes for the whole operating situation.

Fig. 10 demonstrates the emulated virtual inertia power from the ESS for Scenario 4. Clearly, the ESS controlled

TABLE 1. The microgrid control parameters for each scenario.

| Parameter	Scenario 1	Scenario 2	Scenario 3	Scenario 4
Primary control unit				
Governor time constant, T_g (s)	0.1	0.1	0.1	0.1
Turbine time constant, T_t (s)	0.4	0.4	0.4	0.4
Primary droop factor, R (Hz/p.u.MW)	2.4	2.4	2.4	2.4
Secondary control unit				
Secondary frequency controller, K_i (s)	0.2	0.2	0.2	0.2
Frequency bias, β (p.u.MW/Hz)	0.99	0.99	0.99	0.99
Inertia control unit				
Virtual inertia value, J_{VI} (s)	1.6	1.6	1.6	1.6
Virtual damping value, D_{VI} (s)	1.2	1.2	1.2	1.2
Time constant of inverter-based ESS, T_{ESS} (s)	10	10	10	10
Maximum capacity of ESS, $P_{ESS\ max}$ (p.u.MW)	0.3	0.3	0.3	0.3
Minimum capacity of ESS, $P_{ESS\ min}$ (p.u.MW)	-0.3	-0.3	-0.3	-0.3
Renewable control unit				
Time constant of wind turbine, T_{WT} (s)	1.4	1.4	1.4	1.4
Time constant of solar system, T_{PV} (s)	1.9	1.9	1.9	1.9
Microgrid control unit				
System (microgrid) inertia, H (p.u.MW s)	0.082	0.082	0.066 (-20%)	0.016 (-80%)
System (microgrid) damping, D (p.u.MW/Hz)	0.016	0.016	0.012 (-20%)	0.003 (-80%)
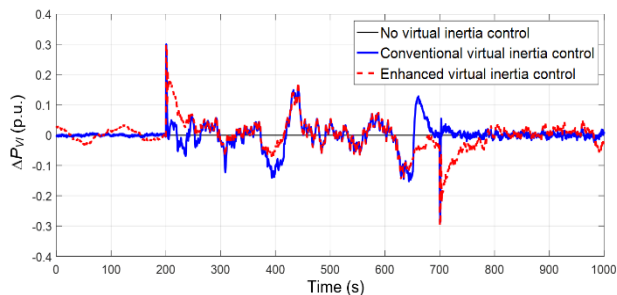
FIGURE 10. Power change of the ESS with virtual inertia and damping emulation for Scenario 4.

by the proposed control technique is effectively charged/discharged in response to the severe disturbances and contingencies.

Accordingly, applying the proposed virtual inertia control not only reduces transient excursion but also shortens the stabilizing/settling time and derives the frequency deviation close to zero, improving the stability and robustness of microgrid operation and control.

V. CONCLUSIONS

In this paper, the novel enhanced modeling of derivative technique-based virtual inertia control has been proposed to imitate virtual damping and inertia simultaneously, improving system inertia, system damping, and frequency stability during the severe disturbances and contingencies. The derivative technique is applied to control the inverter-based ESS in the microgrid for inertia emulation, by calculating the derivative of frequency. The study results are summarized as follows:

1) Eigenvalue investigation has been presented to evaluate the dynamic impacts of virtual damping and virtual inertia over the system performance. It is shown that the side effect of applying the high value of virtual inertia constant is that the system will require a longer time to settle. On the contrary, the side effect of applying the high value for virtual damping is that it can cause a large second overshoot, leading to the degraded system performance. Thus, in applying virtual inertia and virtual damping simultaneously, it is better to keep a smaller value of virtual damping and give the main responsibility of suppressing the frequency deviation in case of the contingency to the virtual inertia part.

2) Time-domain analysis and results report the higher stability/performance of the proposed control technique under different test scenarios including the severe disturbances and high uncertainty situations. Obviously, in the severe situation of high RESs penetration with low system damping and inertia, the cases of conventional virtual inertia control and no inertia control fail to stabilize frequency stability within the acceptable standard owing to the lack of virtual damping emulation, causing system instability and collapse. To handle this problem, the disconnection of RESs unit is required in case of conventional inertia control to avoid the system collapse. On the other hand, the proposed control technique could effectively maintain the frequency within the satisfactory range under the applied disturbances. These results clearly validate the efficiency, resiliency, and robustness of the proposed control technique.

3) The stability study confirms that the coordinated design of virtual inertia and virtual damping is suitable and effective to gain a new trade-off between frequency transient/deviation and settling time of the microgrid. It does not only reduce transient excursion/frequency deviation but also improves the damping performance and withstands the system disturbances without any harmful effect.

Finally, the simultaneous emulation of virtual damping and virtual inertia in the derivative technique-based virtual inertia control for microgrid frequency regulation can be considered as an important outcome of this work. Eventually, the proposed model of virtual inertia control will be useful and essential for further analysis and studies in frequency control respect to virtual inertia and damping emulation capabilities. Besides, it could be implemented to any category of microgrids with different size/complexity.

APPENDIX

The pertinent control parameters of the studied microgrid used in each scenario are listed in Table 1.

REFERENCES

[1] H. Lotfi and A. Khodaei, "Hybrid AC/DC microgrid planning," *Energy*, vol. 118, no. 1, pp. 37–46, 2017.

[2] *Frequency Stability Evaluation Criteria for the Synchronous Zone of Continental Europe: Requirements and Impacting Factors*, European Network of Transmission System Operations for Electricity (ENTSO-E), Brussels, Belgium, 2016.

[3] H.-P. Beck and R. Hesse, "Virtual synchronous machine," in *Proc. 9th Int. Conf. Elect. Power Qual. Utilisation (EPQU)*, Oct. 2007, pp. 1–6.

[4] Y. Chen, R. Hesse, D. Turschner, and H.-P. Beck, "Improving the grid power quality using virtual synchronous machines," in *Proc. Int. Conf. Power Eng. Energy Elect. Drives*, May 2011, pp. 1–6.

[5] Y. Chen, R. Hesse, D. Turschner, and H.-P. Beck, "Investigation of the virtual synchronous machine in the island mode," in *Proc. IEEE PES Innov. Smart Grid Technol. Conf. Eur.*, Oct. 2012, pp. 1–6.

[6] J. Driesen and K. Visscher, "Virtual synchronous generators," in *Proc. 21st Century IEEE Power Energy Soc. Gen. Meeting, Convers. Delivery Elect. Energy (PES)*, Jul. 2008, pp. 1–3.

[7] S. D'Arco, J. A. Suul, and O. B. Fosso, "A virtual synchronous machine implementation for distributed control of power converters in smartgrids," *Electr. Power Syst. Res.*, vol. 122, no. 1, pp. 180–197, 2015.

[8] J. Liu, Y. Miura, and T. Ise, "Comparison of dynamic characteristics between virtual synchronous generator and droop control in inverter-based distributed generators," *IEEE Trans. Power Electron.*, vol. 31, no. 5, pp. 3600–3611, May 2016.

[9] Y. Hirase, K. Sugimoto, K. Sakimoto, and T. Ise, "Analysis of resonance in microgrids and effects of system frequency stabilization using a virtual synchronous generator," *IEEE J. Emerg. Sel. Topics Power Electron.*, vol. 4, no. 4, pp. 1287–1298, Dec. 2016.

[10] J. Alipoor, Y. Miura, and T. Ise, "Stability assessment and optimization methods for microgrid with multiple VSG units," *IEEE Trans. Smart Grid*, vol. 9, no. 2, pp. 1462–1471, May 2018.

[11] H. Wu *et al.*, "Small-signal modeling and parameters design for virtual synchronous generators," *IEEE Trans. Ind. Electron.*, vol. 63, no. 7, pp. 4292–4303, Jul. 2016.

[12] H. Bevrani, T. Ise, and Y. Miura, "Virtual synchronous generators: A survey and new perspectives," *Int. J. Electr. Power Energy Syst.*, vol. 54, pp. 244–254, Jan. 2014.

[13] U. Tamrakar, D. Shrestha, M. Maharjan, B. P. Bhattarai, T. M. Hansen, and R. Tonkoski, "Virtual inertia: Current trends and future directions," *Appl. Sci.*, vol. 7, no. 7, p. 654, 2017.

[14] E. Rakhshani, D. Remon, A. M. Cantarellas, J. M. Garcia, and P. Rodriguez, "Virtual synchronous power strategy for multiple HVDC interconnections of multi-area AGC power systems," *IEEE Trans. Power Syst.*, vol. 32, no. 3, pp. 1665–1677, May 2017.

[15] E. Rakhshani, D. Remon, A. M. Cantarellas, and P. Rodriguez, "Analysis of derivative control based virtual inertia in multi-area high-voltage direct current interconnected power systems," *IET Gener. Transmiss. Distrib.*, vol. 10, no. 6, pp. 1458–1469, Apr. 2016.

[16] E. Rakhshani and P. Rodriguez, "Inertia emulation in AC/DC interconnected power systems using derivative technique considering frequency measurement effects," *IEEE Trans. Power Syst.*, vol. 32, no. 5, pp. 3338–3351, Sep. 2017.

[17] S. M. Alhejaj and F. M. Gonzalez-Longatt, "Impact of inertia emulation control of grid-scale BESS on power system frequency response," in *Proc. Int. Conf. Students Appl. Eng. (ICSAE)*, Oct. 2016, pp. 254–258.

[18] T. Kerdphol, F. S. Rahman, Y. Mitani, K. Hongesombut, and S. Küfeoğlu, "Virtual inertia control-based model predictive control for microgrid frequency stabilization considering high renewable energy integration," *Sustainability*, vol. 9, no. 5, p. 773, 2017.

[19] T. Kerdphol, F. S. Rahman, and Y. Mitani, "Virtual inertia control application to enhance frequency stability of interconnected power systems with high renewable energy penetration," *Energies*, vol. 11, no. 4, pp. 981–997, 2018.

[20] T. Kerdphol, F. S. Rahman, Y. Mitani, M. Watanabe, and S. Küfeoglu, "Robust virtual inertia control of an islanded microgrid considering high penetration of renewable energy," *IEEE Access*, vol. 6, pp. 625–636, 2017.

[21] J. Fang, R. Zhang, H. Li, and Y. Tang, "Frequency derivative-based inertia enhancement by grid-connected power converters with a frequency-locked-loop," *IEEE Trans. Smart Grid*, to be published, doi: 10.1109/TSG.2018.2871085.

[22] X. Xi, H. Geng, and G. Yang, "Small signal stability of weak power system integrated with inertia tuned large scale wind farm," in *Proc. IEEE Innov. Smart Grid Technol.-Asia (ISGT ASIA)*, May 2014, pp. 514–518.

[23] H. Dharmawardena, K. Uhlen, and S. S. Gjerde, "Modelling wind farm with synthetic inertia for power system dynamic studies," in *Proc. IEEE Int. Energy Conf. (ENERGYCON)*, Apr. 2016, pp. 1–6.

[24] H. E. Brown and C. L. DeMarco, "Synthetic inertia and small signal instability," in *Proc. 48th North Amer. Power Symp.*, Sep. 2016, pp. 1–6.

[25] E. Hammad, A. Farraj, and D. Kundur, "On effective virtual inertia of storage-based distributed control for transient stability," *IEEE Trans. Smart Grid*, vol. 10, no. 1, pp. 327–336, Jan. 2019.

[26] J. Fang, P. Lin, H. Li, Y. Yang, and Y. Tang, "An improved virtual inertia control for three-phase voltage source converters connected to a weak grid," *IEEE Trans. Power Electron.*, to be published, doi: 10.1109/TPEL.2018.2885513.

[27] M. H. Fini and M. E. H. Golshan, "Determining optimal virtual inertia and frequency control parameters to preserve the frequency stability in islanded microgrids with high penetration of renewables," *Electr. Power Syst. Res.*, vol. 154, no. 1, pp. 13–22, 2018.

[28] H. Bevrani, *Robust Power System Frequency Control*, 2nd ed. New York, NY, USA: Springer, 2014.

[29] P. Kundur, *Power System Stability and Control*. New York, NY, USA: McGraw-Hill, 1994.

[30] H. Bevrani, M. R. Feizi, and S. Ataee, "Robust frequency control in an islanded microgrid: H∞ and μ-synthesis approaches," *IEEE Trans. Smart Grid*, vol. 7, no. 2, pp. 706–717, Mar. 2016.

[31] J. Pahasa and I. Ngamroo, "PHEVs bidirectional charging/discharging and SoC control for microgrid frequency stabilization using multiple MPC," *IEEE Trans. Smart Grid*, vol. 6, no. 2, pp. 526–533, Mar. 2015.

[32] J. Pahasa and I. Ngamroo, "Coordinated control of wind turbine blade pitch angle and PHEVs using MPCs for load frequency control of microgrid," *IEEE Syst. J.*, vol. 10, no. 1, pp. 97–105, Mar. 2016.

[33] R. Panel, "Stage one final determination: Review of the frequency operating standard," Austral. Energy Market Commission, Sydney, NSW, Australia, Tech. Rep. REL0065, 2017.

THONGCHART KERDPHOL (S'14–M'16) received the B.Eng. and M.Eng. (Hons.) degrees in electrical engineering from Kasetsart University, Bangkok, Thailand, in 2010 and 2012, respectively, and the Ph.D. degree in electrical and electronic engineering from the Kyushu Institute of Technology (Kyutech), Kitakyushu, Japan, in 2016. From 2016 to 2017, he was a Postdoctoral Fellow with the Department of Electrical and Electronic Engineering, Kyutech. In 2018, he was a Visiting Researcher with the Institute of Electrical Power Engineering and Energy Systems, Clausthal University of Technology, Clausthal-Zellerfeld, Germany.

He is currently a Senior Research Fellow with the Power System and Renewable Energy Laboratory (Mitani-Watanabe Lab), Kyutech. His research interests include power system stability, robust power system control, intelligent optimization, and smart/micro-grid control.

FATHIN SAIFUR RAHMAN (S'15) received the B.Sc. degree in electrical power engineering and the M.Sc. degree in electrical engineering from the Institut Teknologi Bandung, Indonesia, in 2012 and 2013, respectively.

He is currently pursuing the Ph.D. degree in electrical and electronic engineering with the Mitani-Watanabe Laboratory, Kyushu Institute of Technology, Fukuoka, Japan. His research interests include power system stability, smart grid and clean energy, optimization in power systems, and application of synchrophasor in power systems.

MASAYUKI WATANABE (S'03–M'05) received the B.Sc., M.Sc., and Dr.Eng. degrees in electrical engineering from Osaka University, Japan, in 2001, 2002, and 2004, respectively.

He is currently an Associate Professor with the Department of Electrical and Electronic Engineering, Kyushu Institute of Technology, Fukuoka, Japan. He has authored books/book chapters and over 100 journal/conference papers. His research interest includes the area of analysis of power systems.

YASUNORI MITANI (M'87) received the B.Sc., M.Sc., and D.Eng. degrees in electrical engineering from Osaka University, Japan, in 1981, 1983, and 1986, respectively. From 1994 to 1995, he was a Visiting Research Associate with the University of California at Berkeley, Berkeley, CA, USA. From 2016 to 2018, he was the President of the Institute of Electrical Engineers of Japan, Power and Energy Society.

He is currently the Vice President and a Professor with the Department of Electrical and Electronic Engineering and the Director of the Industry-Academic Collaboration Division, Kyushu Institute of Technology, Fukuoka, Japan. He has authored numerous books/book chapters and over 250 journal/conference papers. His research interests include the areas of power system stability, dynamics, and control.

DIRK TURSCHNER received the Diploma degree in electrical engineering from the Braunschweig University of Technology, in 1993, and the Dr.Ing. degree in electrical engineering from the Clausthal University of Technology (TU Clausthal), Clausthal-Zellerfeld, Germany, in 2002.

He is currently an Assistant Professor and the Head of the Department of Power Mechatronics and Drives, Institute of Electrical Power Engineering and Energy Systems, TU Clausthal. His research interests include virtual synchronous machine, field-oriented control of electrical drives, mechanical and electric oscillation damping, mechanical test beds, programmable logic control, and development of power electronic circuits.

HANS-PETER BECK was born in Ehmen, Wolfsburg, Germany, in 1947. He received the Dr.Ing. degree in electrical engineering from the Berlin University of Technology, Berlin, Germany, in 1981.

He is currently a Professor and the Director of the Institute of Electrical Power Engineering and Energy Systems, Clausthal University of Technology, Clausthal-Zellerfeld, Germany. He has authored over 50 journal/conference papers. His research interests include power mechatronics, electrical energy conditioning, energy management systems, virtual synchronous machine, gas network simulation, and energy system technology.

• • •